X-ray structures along the reaction pathway of cyclodextrin glycosyltransferase elucidate catalysis in the α-amylase family

Uitdehaag, Joost C.M.; Mosi, Renée; Kalk, Kor H.; Veen, Bart A. van der; Dijkhuizen, Lubbert; Withers, Stephen G.; Dijkstra, Bauke W.

Published in:
Nature Structural Biology

DOI:
10.1038/8235

line using an ADSC Quantum4 CCD detector and processed using MOSFLM[25]. Molecular replacements were performed with AMORE[26], ncs averaging of electron density was performed with DPHASE (G.V., unpublished) and model building was peformed in O[27]. Heavy atom refinement, isomorphous difference phasing, and combination with molecular replacement phases for apoArgRBst were performed in a modified version of MLPHARE[28]. Both structures were refined using X-PLOR, with tightly restrained thermal parameters and a bulk solvent correction[29]. For apoArgRBst, ncs restraints were applied separately to backbone atoms of the DBDs (residues 4–51) and the core domains (71–149), but not to the β-fingers of the DBDs (52–64) or the linkers (65–70), which showed variability among subunits. All ϕ,ψ angles for both structures map to favored and additional allowed regions of the Ramachandran plot, as defined in PROCHECK[30]. Crystallographic data and results are summarized in Table 1.

Coordinates. Coordinates for ArgRBst and ArgRBst-C have been deposited in the Protein Data Bank (accession codes 1B4A and 1B4B, respectively).

Acknowledgments
We thank the staff of the CHESS F1 beamline for synchrotron support, F. Guo and M. Gopaul for assistance with data collection, and X. Li for help in crystallization. We also acknowledge helpful comments and discussions from M. Lemmon, H. Lu, H. Nelson, M. Lewis, and W.K. Maas. Supported by a grant from the National Institutes of Health to G.V.

Correspondence should be addressed to G.V.
email: vanduyne@mail.med.upenn.edu

Received 8 October, 1998; accepted 22 December, 1998.

1. Glansdorff, N. in *Escherichia coli and Salmonella: cellular and molecular biology.* (ed. Neidhardt, F.C.) 408–433 (American Society for Microbiology Press, Washington, D.C.; 1996).
2. Maas, W.K. *Microbiol. Rev.* **58**, 631–640 (1994).
3. Czaplewski, L.G., North, A.K., Smith, M.C.M., Baumberg, S. & Stockley, P.G. *Mol. Microbiol.* **6**, 267–275 (1992).
4. Stirling, C.J., Szatmari, G., Stewart, G., Smith, M.C. & Sherratt, D.J. *EMBO J.* **7**, 4389–4395 (1988).
5. Lim, D.B., Oppenheim, J.D., Eckhardt, T. & Maas, W.K. *Proc. Natl. Acad. Sci. USA* **84**, 6697–701 (1987).
6. North, A.K., Smith, M.C. & Baumberg, S. *Gene* **80**, 29–38 (1989).
7. Lu, C.D., Houghton, J.E. & Abdelal, A.T. *J. Mol. Biol.* **225**, 11–24 (1992).
8. Dion, M. *et al. Mol. Microbiol.* **25**, 385–398 (1997).
9. Fleischmann, R.D. *et al. Science* **269**, 496–512 (1995).
10. Cole, S.T. *et al. Nature* **393**, 537–544 (1998).
11. Rodríguez-García, A., Ludovice, M., Martín, J.F. & Liras, P. *Mol. Microbiol.* **25**, 219–228 (1997).
12. Tian, G. & Maas, W.K. *Mol. Microbiol.* **13**, 599–608 (1994).
13. Burke, M., Merican, A.F. & Sherratt, D.J. *Mol. Microbiol.* **13**, 609–618 (1994).
14. Van Duyne, G.D., Ghosh, S., Maas, W.K. & Sigler, P.B. *J. Mol. Biol.* **256**, 377–391 (1996).
15. Grandori, R. *et al. J. Mol. Biol.* **254**, 150–162 (1995).
16. Chen, S.H., Merican, A.F. & Sherratt, D.J. *Mol. Microbiol.* **24**, 1143–1156 (1997).
17. Sunnerhagen, M., Nilges, M., Otting, G. & Carey, J. *Nature Struct. Biol.* **4**, 819–826 (1997).
18. Brennen, R.G. *Cell* **74**, 773–776 (1993).
19. Tian, G., Lim, D., Oppenheim, J.D. & Maas, W.K. *J. Mol. Biol.* **235**, 221–230 (1994).
20. Wang, H., Glansdorff, N. & Charlier, D. *J. Mol. Biol.* **277**, 805–824 (1998).
21. Tian, G., Lim, D., Carey, J. & Maas, W.K. *J. Mol. Biol.* **226**, 387–397 (1992).
22. Charlier, D. *et al. J. Mol. Biol.* **226**, 367–386 (1992).
23. Schultz, S.C., Shields, G.C. & Steitz, T.A. *Science* **253**, 1001–1007 (1991).
24. Miller, C.M., Baumberg, S. & Stockley, P.G. *Mol. Microbiol.* **26**, 37–48 (1997).
25. Abrahams, J.P. & Leslie, A.G.W. *Acta Crystallogr. D* **52**, 30–42 (1996).
26. Navaza, J. *Acta Crystallgr. A* **50**, 157–163 (1994).
27. Jones, T.A., Zou, J.Y., Cowan, S.W. & Kjeldgaard, M. *Acta Crystallogr. A* **47**, 110–119 (1991).
28. Otwinowski, Z. In *CCP4 Proceedings.* 80–88 (Daresbury Laboratory, Warrington, UK, 1991).
29. Jiang, J.S. & Brunger, A.T. *J. Mol. Biol.* **243**, 100–115 (1994).
30. Laskowski, R.A., MacArthur, M.W., Moss, D.S. & Thornton, J.M. *J. Appl. Crystallogr.* **26**, 283–291 (1993).
31. Kraulis, P. *J. Appl. Crystallogr.* **24**, 946–950 (1991).
32. Merritt, E.A. & Bacon, D.J. *Methods Enzymol.* **277**, 505–524 (1997).
33. Carson, M. *J. Appl. Crystallgr.* **24**, 958–961 (1991).

X-ray structures along the reaction pathway of cyclodextrin glycosyltransferase elucidate catalysis in the α-amylase family

Joost C. M. Uitdehaag[1], Renée Mosi[2], Kor H. Kalk[1], Bart A. van der Veen[3], Lubbert Dijkhuizen[3], Stephen G. Withers[2] and Bauke W. Dijkstra[1]

[1]BIOSON Research Institute, Groningen Biomolecular Sciences and Biotechnology Institute (GBB) and Laboratory of Biophysical Chemistry, Nijenborgh 4, 9747 AG Groningen, University of Groningen, the Netherlands. [2]Department of Chemistry, University of British Columbia, Vancouver, British Columbia, Canada V6T 1Z1. [3]Department of Microbiology, Kerklaan 30, 9751 NN Haren, GBB Institute, University of Groningen, the Netherlands.

Cyclodextrin glycosyltransferase (CGTase) is an enzyme of the α-amylase family, which uses a double displacement mechanism to process α-linked glucose polymers. We have determined two X-ray structures of CGTase complexes, one with an intact substrate at 2.1 Å resolution, and the other with a covalently bound reaction intermediate at 1.8 Å resolution. These structures give evidence for substrate distortion and the covalent character of the intermediate and for the first time show, in atomic detail, how catalysis in the α-amylase family proceeds by the concerted action of all active site residues.

Ever since the structure of lysozyme was determined[1], the enzyme mechanisms of glycosyl hydrolases and transferases have aroused wide interest[2–4]. Using similar chemical principles, these enzymes process a wide variety of carbohydrate polymers, many of which are important as nutrients, cell wall components or signal transmitters[5]. Glycosyl hydrolases and transferases employ four basic mechanisms, named according to the anomeric configuration of the substrate (α or β-glycosidic bonds) and the stereochemical outcome of the reaction (retention or inversion)[4]. The β-retaining mechanism of hen egg white lysozyme is a well-known example[6,7]. The α-retaining mechanism is used by enzymes from the α-amylase family (glycosyl hydrolase family 13; ref. 5), such as α-amylase, pullulanase, iso-amylase and cyclodextrin glycosyltransferase (CGTase), which all share a virtually identical catalytic site architecture[8,9].

The α-retaining mechanism is a double displacement process, which proceeds in two steps (Fig. 1)[4,10]. In the first step, CGTase cleaves an α(1–4) glycosidic bond in its substrate, starch, and forms a covalent β(1–4)-linked glycosyl-enzyme intermediate[11]. In the second step, the covalent bond of the intermediate is cleaved and an α(1–4) glycosidic bond is reformed with an acceptor, such as water or the OH-4 group (the hydroxyl group at position 4) of another sugar residue. CGTase is unique in its ability to use the free hydroxyl at the non-reducing end of the intermediate

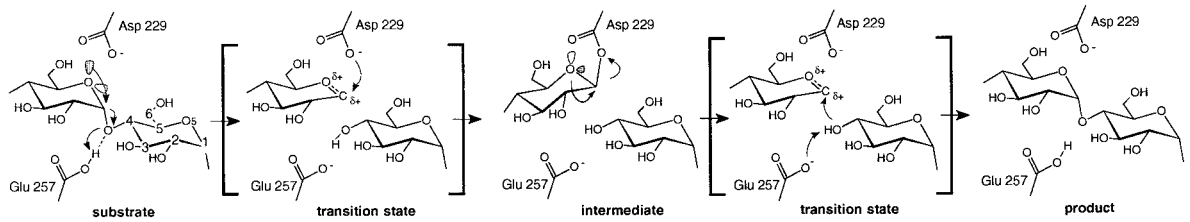

Fig. 1 Scheme of the CGTase reaction mechanism. The first step, leading to intermediate formation, is explained in the text. In the second step, Glu 257 activates an acceptor that subsequently reacts with the intermediate, leading to product formation. This proceeds with a mechanism that is essentially the reverse of the first step. The glucoside ring atom nomenclature is incorporated in the left-most picture. The shaded orbital represents the electrons that are in a proper orientation to participate in the cleavage of the substrate α-glycosidic bond according to the stereo-electronic theory[22]. However, when the intermediate β-glycosyl-enzyme bond is cleaved, such a correctly oriented orbital is not present, as pointed out in the text.

sugar chain as an acceptor, thus forming a cyclic oligoglucoside, a cyclodextrin. Both steps of the mechanism go through high-energy oxocarbenium-like transition states[4], in which the reaction center of the sugar is planar and positively charged[12]. Two active site amino acids play distinct roles in catalysis. One is the acid/base Glu 257, which protonates the glycosidic oxygen of the scissile bond in the first step, and then deprotonates the attacking OH group in the second step. The other is the nucleophile, Asp 229, which attacks the sugar, forming the covalent linkage within the intermediate[11] (Fig. 1). Other residues in the catalytic sites of α-amylase family members aid in the catalytic process, as evidenced by their evolutionary conservation and as corroborated by extensive mutagenesis experiments[9].

Our work on cyclodextrin glycosyltransferase (CGTase) has resulted in the first set of X-ray structures in which a natural substrate (Fig. 2) and a covalent intermediate (Fig. 3) are competently bound in the active site of a member of the α-amylase family. These structures reveal the complexities of the α-retaining mechanism, and show how active site residues are involved in substrate distortion and induced fit mechanisms, for which they make exquisite use of known sugar chemistry.

How CGTase binds its substrate

We have freeze-trapped a maltononaose oligosaccharide chain in the active site of the inactive CGTase mutant E257Q/D229N (Table 1). The maltononaose chain is bound from subsites -7 to +2 in a manner analogous to that of a previously determined pseudo-nonasaccharide inhibitor complex at 2.6 Å resolution[13,14]. However, the catalytic subsite (labeled -1) now contains a competent substrate, with an intact scissile bond, instead of a valienamine inhibitor sugar unit[14]. The substrate bound from subsites -2 to +1 is shown in Fig. 2. The electron density in the active site shows that the sugar in the catalytic subsite (-1) is clearly distorted, flattening the C2-C1-O5-C5 torsion angle. This torsion angle is -63° in the $^4C_1$ chair minimum energy conformation[15], and -44° in the substrate complex, whereas it would be 0° in the transition state (Fig. 1). The distortion is caused, at least in part, by residues Asp 328 and His 140 (Fig. 4), as best seen by overlaying the substrate at subsite -1 with the glucose $^4C_1$ chair conformation[15] (Fig. 2). When the glucose C3, C4 and C5 atoms are used as the basis for superposition, His 140 is seen to form a buried hydrogen bond with the O6 residue of the sugar residue in subsite -1. However there would be severe van der Waals clashes between Asp 328 and the glucose O2 atom (<<1.8 Å) if the sugar in this site were undistorted (Fig. 4). When we compare the CGTase structure with bound substrate to that of the uncomplexed wild-type structure[16] determined under similar experimental conditions, we observe an induced fit for several residues that reorient to bind and activate the substrate (Fig. 4). His 140 flips its ring (according to the hydrogen bond networks) and Glu(Gln) 257 rotates to interact with the scissile bond oxygen[13]. This rotation creates space for Arg 227 to change conformers, enabling it to bind simultaneously to the nucleophile Asp(Asn) 229 and the substrate OH-2 group, the latter being the most contacted group in the catalytic subsite (Fig. 4).

The importance of strong hydrogen bonds to the substrate OH-2 hydroxyl group in glycosidase catalysis has been demonstrated previously[17]. Hydrogen bonding interactions at this position can contribute up to 48 kJ mol^{-1} to transition state stabilization[18,19]. These hydrogen bonds serve two purposes. One is the distortion of the sugar ring towards the half chair conformation. The other is a reduction in the electronegativity of the 2-hydroxyl, which otherwise strongly disfavors formation of a positively charged transition state[18,19]. CGTase reduces this electronegativity in two ways. First, the OH-2 hydroxyl donates a strong hydrogen bond (2.7 Å) to Asp 328 (Fig. 4), leading to an $O2^{\delta-}\cdots H2^{\delta+}$ charge separation, which negatively polarizes the O2 atom. This effect might explain why the D328N mutation[16], which remains capable of ring distortion, still decreases the activity of CGTase 56,000-fold[16]. Secondly, the partial negative charge on the O2 atom can be stabilized by the positive charges of the nearby basic residues His 327 and Arg 227, thereby explaining the counter-intuitive presence of basic residues in an active site that binds a positively charged transition state. Both effects provide an example of charge redistribution (electronic distortion) within the substrate, facilitating formation of oxocarbenium ion-like transition states and hence the formation of the covalent intermediate.

How CGTase binds its covalent intermediate

A 4-deoxy maltotriosyl moiety covalently bound to the nucleophile Asp 229 of E257Q CGTase was cryo-crystallographically trapped by use of 4-deoxymaltotriosyl α-fluoride[11] (Table 1). This compound both promotes intermediate formation because fluoride is a good leaving group, and simultaneously prevents intermediate breakdown because no hydroxyl group at position four is available to act as acceptor for transglycosylation[11]. The intermediate trapped in this fashion has no unnatural chemical substitutions on the sugar in the catalytic site -1 (refs 2,7) and shows an unequivocal β-glycosidic covalent bond between the Asp 229 Oδ1 atom and the substrate anomeric C1 atom (Fig. 3). Taken together with NMR and mass-spectrometric evidence for a covalent intermediate in the α-amylase family (see ref. 11 for an overview), this result definitively shows that the *intermediate* in the α-retaining mechanism is not a charged oxocarbenium ion[4]. Previously, one of

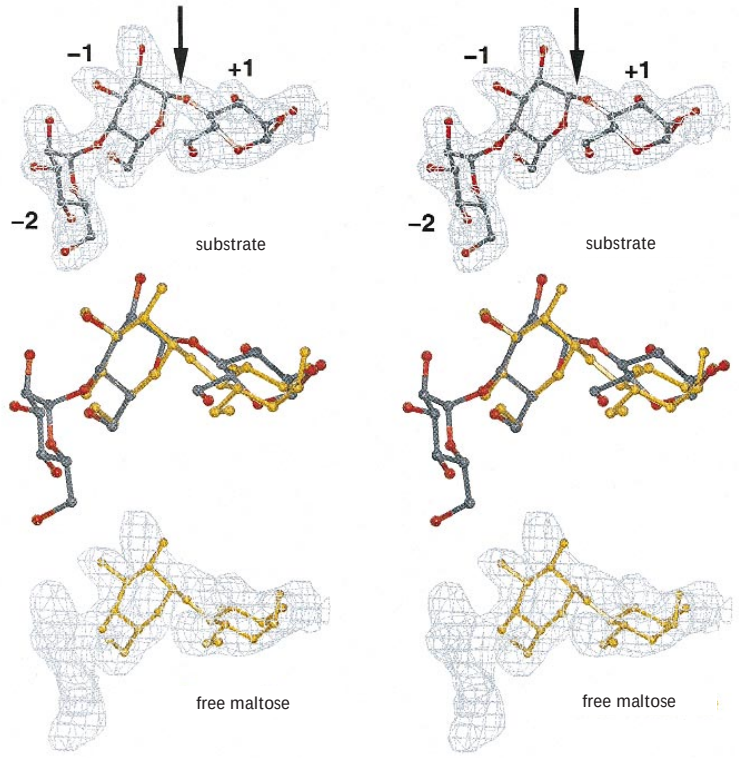

Fig. 2 Stereoview of the substrate bound to CGTase. The maltononaose binds from subsites -7 to +2, but for clarity only subsites -2, -1 and +1 are shown. The arrow indicates the scissile bond. ***a***, Showing how the substrate fits into the $2F_o$ - F_c electron density (1σ contoured), which was calculated with F_c and phases from unliganded CGTase to avoid bias[16]. ***b***, The substrate distortion at the catalytic subsite -1 (central sugar ring) is revealed by superposition with the minimum energy conformation of maltose (orange)[15]. The superposition is based on the glucose C3, C4 and C5 atoms in subsite -1. Comparing the substrate ring puckering parameters with a potential map from molecular mechanics calculations indicates that the glucose ring at the catalytic subsite is strained by ~17 kJ mol^{-1} and has a $^4C_1$ chair conformation distorted towards a $^2H_3$ half chair[15]. ***c***, Undistorted (free) maltose clearly does not fit the $2F_o$ - F_c electron density at subsite -1. The glycosidic bond torsion angles of maltose were adjusted to fit the density at subsite +1.

the arguments in favor of an oxocarbenium intermediate in both α- and β-retaining mechanisms was the large distance between the nucleophilic residue and the substrate[8,20]. However, this distance was not much greater than the sum of the van der Waals radii of the atoms involved. Indeed, as we observe, this distance is overcome by a 2 Å shift of the glucose ring when compared to the substrate (Figs 3, 4). In this new position the intermediate is bound in an undistorted $^4C_1$ chair conformation (Fig. 3 legend). The Asp 229 Oδ2 carbonyl oxygen is unfavorably close (2.7 Å) to the intermediate O5 atom, and the contact to His 140 is lost, but the intermediate is stabilized by improved geometry of the hydrogen bonds to Arg 227 and His 327, and good stacking interactions[21] with Tyr 100 (Fig. 4). Moreover, the residue Asp 328 appears to have followed the shift of the glucose ring, retaining its hydrogen bonds with the sugar O2 and O3 atoms in the intermediate structure (Fig. 4).

This minimum energy $^4C_1$ chair conformation of the intermediate is interesting for two reasons. First, it suggests that stereo-electronic assistance is not an important factor for this step, since that would require a distortion towards a $^{1,4}B$ boat conformation in order to align the lone pair of the ring oxygen with the enzyme-intermediate glycosidic bond[22]. Secondly, there is no sign of distortion towards the half chair of the transition state such as that observed for the bound substrate. Undistorted intermediates have also been seen in several β-retaining enzymes[2,7]. The lack of distortion indicates that the catalytic subsite -1 is stereochemically complementary to the intermediate, similar to a situation also seen in, for example, the sulfur transferase rhodanese[23].

Such complementarity could be needed to compensate for the intermediate's being inherently more unstable than the substrate, since the carboxylate of Asp 229 is a much better leaving group than the sugar OH-4 group at subsite +1 (ref. 24). Favorable interactions could prolong the lifetime of the intermediate, which would prevent an unproductive re-formation of the substrate, and allow time for a new acceptor to diffuse into the active site. In such a way catalysis is accomplished by increasing the chances of a productive reaction cycle. Possibly, this could combine with an induced fit-like mechanism, in which acceptor binding at subsite +1 introduces distortion of the intermediate.

Mechanism of the first reaction step

Comparison of the crystal structures of free enzyme[16], substrate bound enzyme and the CGTase with covalent intermediate, gives a clear picture of how catalysis of the first reaction step of CGTase proceeds (Fig. 4). To start, the substrate binds, and at subsite -1 the glucose ring becomes distorted. For α-amylases, substrate binding at subsite -1 is indeed energetically unfavorable[25]. Conceivably, Asp 328 pushes the substrate O2 atom towards the intermediate position, while His 140 is firmly holding the sugar O6 atom (Fig. 4). The substrate displaces the central water molecule indicated in Fig. 4, allowing His 327 and Arg 227 to bind to

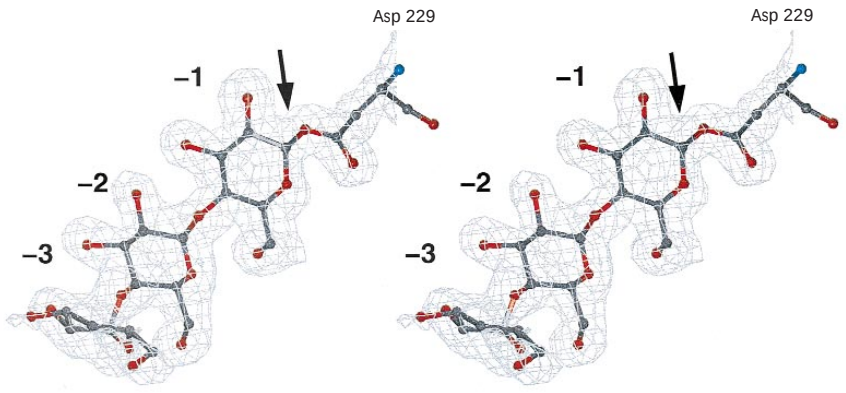

Fig. 3 Stereoview of the covalent intermediate electron density from a $2F_o$ - F_c omit[37] map (1σ contoured), the arrow indicates the glycosyl–enzyme covalent bond. In contrast to earlier work with other enzymes, neither the nucleophilic amino acid nor the glucose at the catalytic subsite -1 has been chemically modified[2,7]. Comparing the intermediate ring puckering parameters with those of small molecule X-ray structures and a potential map from molecular mechanics calculations indicates that the sugar bound to Asp 229 has a low-energy $^4C_1$ chair conformation[15].

the substrate O2 atom and Glu(Gln) 257 to form a hydrogen bond with the scissile bond oxygen. Simultaneously, Arg 227 interacts with the *anti*-oriented lone pair orbital of Asp(Asn) 229, thereby orienting the nucleophile. The more basic *syn* orbital[20] then attacks the C1 atom of the sugar at subsite -1, the transition state[12] for this first step being stabilized electronically by the negative potential that reigns in the catalytic site[26], possibly assisted by the partial negative charge of the π-cloud in the aromatic ring of Tyr 100[27]. In addition, the proximity of the carbonyl oxygen of Asp 229 to the glucose ring O5 atom (as observed in the intermediate structure) may ensure a favorable interaction during transition state formation, when Asp 229 bears a partial negative charge, and O5 a partial positive charge.

Driving forces for the transformation of substrate via transition state into intermediate are provided by the relaxation of the distorted substrate $^4C_1$ chair conformation, the improvement of hydrogen bonds to His 327 and Arg 227, and stacking interactions to Tyr 100 (Fig. 4). In addition, an interaction network involving Trp 75, Asp 135 and Tyr 100 (all conserved in the α-amylase family) tightens itself in the intermediate structure (Fig. 4; Tyr 100 is displaced by ~1.5 Å), and may thus be involved in pulling the glucose ring at subsite -1 towards the intermediate position. Flexibility in the active site is also shown by the loop containing residues 324–334. In the unliganded CGTase and the substrate complex, this loop is in a similar position, but in the intermediate structure the loop is displaced ~0.5 Å towards the glucose ring in subsite -1 (Fig. 4). This flexible loop holds Asp 328 and His 327, residues that appear to contribute to substrate distortion and intermediate binding, and it is possible that the loop assists in these processes by holding these residues and steering them in the appropriate direction.

In addition to the bond-cleavage machinery, individual α-amylase family enzymes have also developed mechanisms that constitute their specificities such as the unique cyclodextrin-forming capability of CGTases. The source of this specificity will be the focus of future work. However, the studies presented here confirm that catalysis is the result of a subtle interplay of many conserved residues that serve to stabilize transition states and reactive intermediates through a network of highly refined interactions.

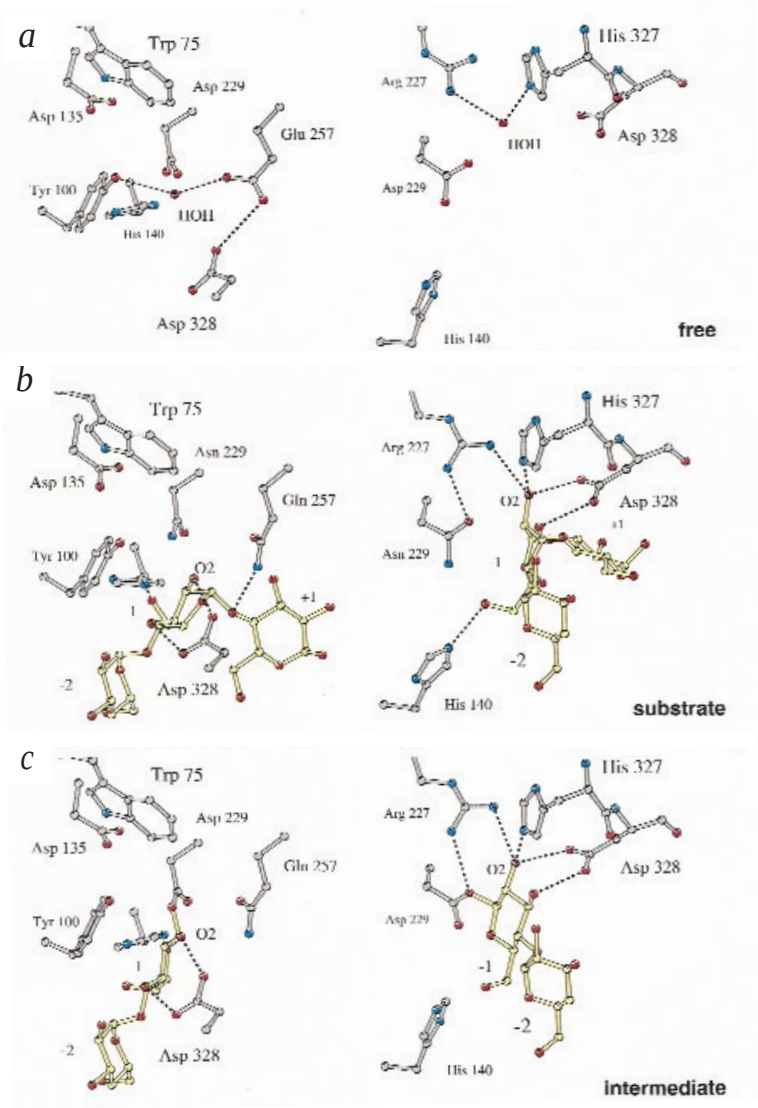

Fig. 4 Structures of the stable states along the reaction coordinate. Two orientations are displayed that can easily be related by focusing on residue Asp 328 and its hydrogen bonds. In the catalytic subsite -1, O2 signifies the substrate's strongly bound hydroxyl group at position 2. ***a***, A 2.2 Å structure of uncomplexed free *Bacillus circulans* strain 251 CGTase at 120 K and pH 7.6[16]. ***b***, The twist in the substrate chair is seen on the left. If undistorted, it would either clash with Asp 328 or not form a hydrogen bond with His 140 (as explained in the text). ***c***, The intermediate chair conformation is presented on the left. This figure was prepared using MOLSCRIPT[39].

Methods

The substrate complex. A crystal of *Bacillus circulans* strain 251 E257Q/D229N CGTase, grown in the presence of 5% (w/v) maltose[16], was washed repeatedly in a mother liquor of 60% (v/v) 2-methyl-2,4-pentanediol (MPD), buffered at stepwise increasing pH, finishing at 100 mM 3-[cyclohexylamino]-1-propanesulfonic acid (CAPS), pH 10.3. Subsequently, the crystal was transferred to 1 ml of fresh mother liquor of pH 10.3, to which ~1 mM β-cyclodextrin (7 glucose units) had been added. After 90 min soaking at room temperature, the crystal was frozen to 120 K for data collection (Table 1). The soaking solution itself served as cryoprotectant. Electron density clearly indicated the presence of maltononaose rather than a β-cyclodextrin bound in the active site. Since the E257Q/D229N mutant still has some activity (0.0004 units mg^{-1} at pH 6.0, compared to 280 units mg^{-1} for wild type CGTase)[16], the maltononaose presumably resulted from transglycosylation of β-cyclodextrin and maltose from the crystallization setup, which could have remained at any of the three carbohydrate binding patches in CGTase[16].

The covalent intermediate. To trap the intermediate, 4-deoxymaltotriosyl α-fluoride (4DG3αF) was used. From this compound the fluoride group leaves easily in the first step of the double displacement reaction (Fig. 1), leading to formation of the intermediate. Degradation of the intermediate by transglycosylation in the second reaction step is prevented through the absence of an acceptor OH-4 group[11]. Instead, water has to be used by CGTase in an hydrolysis reaction, which is slow in CGTase[28]. To further delay intermediate breakdown, activation of water by Glu 257 is prevented by the mutation E257Q[11]. However, crystals of the *Bacillus circulans* strain 251 E257Q CGTase grow in the presence of 5% (w/v) maltose which is a very good acceptor[16]. As pointed out above, simple washing of the crystals does not sufficiently remove this maltose. Therefore, we

sought to replace all bound maltose with 4-deoxymaltose by repeatedly washing a E257Q CGTase crystal in a mother liquor containing 1% (w/v) 4-deoxymaltose over 3 days. This crystal was soaked for 16 min at room temperature in a freshly prepared solution of 60% (v/v) MPD, 100 mM MES (2-[N-morpholino]ethanesulfonic acid) buffer, pH 6.1 and 125 mM 4DG3αF, after which it was frozen to 100 K for data collection (Table 1).

Data reduction and refinement. The substrate data were processed using MADNES[29], the intermediate data using DENZO[30]. Refinement of both structures was performed using a standard approach[28] using O[31] and TNT[32], stereochemistry was analyzed by PROCHECK[33], and WHAT_CHECK[34]. Ideal geometry for the sugars and the β-glycosyl enzyme bond was derived from the crystal structures of maltose and cellobiose[35]. The restraints on sugar bond lengths and bond angles were varied during refinement, but torsion angles were always left unrestrained. No significant variations in sugar geometry were observed, indicating that the diffraction data unambiguously defined the sugar conformations, as also shown by the electron density maps (Figs 2, 3). The substrate and intermediate structures with a minimal R_{free}[36] and least deviating from overall standard geometry were chosen as definitive (Table 1). Electron density maps were calculated with BIOMOL software, using the omit[37] and SIGMAA[38] procedures.

Table 1 Data statistics and final model quality

Data collection	substrate[1]	intermediate[2]
Spacegroup	$P2_12_12_1$	$P2_12_12_1$
Cell axes a, b, c (Å)	117.1, 110.9, 67.6	117.1, 109.3, 65.3
Resolution range (Å)	22.9–2.09	58.5–1.81
No. of unique reflections	45,159	73,264
R_{merge} (%)[3]	6.7	5.3
Completeness (%)	84.9	94.9
Completeness (%) in the last resolution shell (Å)	27.6 (2.16–2.09)	49.9 (1.83–1.81)
Refinement statistics		
No. of amino acids	686 (all)	686 (all)
Active site ligand	maltononaose	4-deoxy maltotriose
MBS1 ligand[4]	maltotetraose	4-deoxy maltotriosyl α-fluoride
MBS2 ligand[4]	maltotetraose	4-deoxy maltose
MBS3 ligand[4]	maltose	4-deoxy maltotriosyl α-fluoride
No. of solvent sites	633	669
Average B factor (Å^2)	13.7	17.7
Final R-factor (%)[5]	15.8	15.5
Final R_{free} (%)[6]	21.7	19.0
R.m.s. deviations from ideal geometry		
Bond lengths (Å)	0.005	0.006
Van der Waals contacts (Å)	0.010	0.012
B-factor correlations (Å^2)	1.387	1.566

[1]X-ray source was rotating anode with Fast area detector.
[2]X-ray source was the EMBL beamline BW7B DESY Hamburg
[3]$R_{merge} = \Sigma_h\Sigma_i|I(h) - I_i(h)|/\Sigma_h\Sigma_i I_i(h)$ where reflection h has intensity $I_i(h)$ on occurrence i and mean intensity I(h).
[4]MBS1-3 are carbohydrate binding patches on the enzyme (MBS = maltose binding site)[16].
[5]R-factor = $\Sigma_h|F_o - F_c|/\Sigma_h F_o$ where F_o and F_c are the observed and calculated structure factor amplitudes of reflection h, respectively.
[6]The R_{free} is calculated as the R-factor, using F_o that were excluded from the refinement (5% of the data)[36].

Verification of the results. To exclude effects of pH, mutations or temperature from the comparison of substrate and intermediate structures, we determined unliganded E257Q/D229N CGTase structures at 120 K both at pH 10.3 and 6.1 (data not shown). No conformational differences due to the pH difference were observed. Moreover, the mutations in the unliganded E257Q/D229N structures are isomorphous with unliganded wild type CGTase at 120 K and pH 7.6[16]. Furthermore, unliganded wild type CGTases at room temperature and 120 K are analogous[16], indicating that studies at 120 K can be relevant for reactivity at room temperature. For further comparisons involving unliganded CGTase, we used the published wild type CGTase structure at 120 K and pH 7.6 (ref. 16; Fig. 4).

Coordinates. Atomic coordinates and structure factor amplitudes have been deposited in the Protein Data Bank (accession codes: 1cxk for the substrate and 1cxl for the intermediate).

Acknowledgments
Our thanks go to M. Dowd for ascertaining the true conformations of substrate and intermediate, and to T. Lindhorst for synthesizing 4-deoxymaltose. This work was supported by the EC grant entitled Structure-function relationships of glycosyltransferases.

Received 17 November, 1998; accepted 19 February, 1999.

1. Blake, C.C.F. *et al. Nature* **206**, 757–761 (1965).
2. White, A. & Rose, D.R. *Curr. Opin. Struct. Biol.* **7**, 645–651 (1997).
3. Sinnott, M.L. *Chem. Reviews* **90**, 1171–1202 (1990).
4. McCarter, J.D. & Withers, S.G. *Curr. Opin. Struct. Biol.* **4**, 885–892 (1994).
5. Henrissat, B. & Davies, G. *Curr. Opin. Struct. Biol.* **7**, 637–644 (1997).
6. Stryer, L. *Biochemistry* (W.H. Freeman, New York; 1988).
7. Davies, G. *et al. Biochemistry* **37**, 11707–11713 (1998).
8. Svensson, B. *Plant. Mol. Biol.* **25**, 141–157 (1994).
9. Janecek, S. *Prog. Biophys. Molec. Biol.* **67**, 67–97 (1997).
10. Koshland, D.E. *Biol. Rev. Camb. Philos. Soc.* **28**, 416–436 (1953).
11. Mosi, R., He, S., Uitdehaag, J., Dijkstra, B.W. & Withers, S.G. *Biochemistry* **36**, 9927–9934 (1997).
12. Tanaka, Y., Wen, T., Blanchard, J.S. & Hehre, E.J. *J. Biol. Chem.* **269**, 32306–32312 (1994).
13. Strokopytov, B. *et al. Biochemistry* **34**, 2234–2240 (1995).
14. Mosi, R. *et al. Biochemistry* **37**, 17192–17198 (1998).
15. Dowd, M.K., French, A.D. & Reilly, P.J. *Carbohydr. Res.* **264**, 1–19 (1994).
16. Knegtel, R.M.A. *et al. J. Biol. Chem.* **270**, 29256–29264 (1995).
17. Namchuk, N.M. & Withers, S.G. *Biochemistry* **34**, 16194–16202 (1995).
18. McCarter, J.D., Adam, M.J. & Withers, S.G. *Biochem. J.* **286**, 721–727 (1992).
19. Braun, C., Brayer, G.D. & Withers, S.G. *J. Biol. Chem.* **270**, 26778–26781 (1995).
20. Strynadka, N.C.J. & James, M.N.G. *J. Mol. Biol.* **220**, 401–424 (1991).
21. Strokopytov, B. *et al. Biochemistry* **35**, 4241–4249 (1996).
22. Sulzenbacher, G., Driguez, H., Henrissat, B., Schülein, M. & Davies, G.J. *Biochemistry* **35**, 15280–15287 (1996).
23. Ploegman, J., Drent, G., Kalk, K. & Hol, W. *J. Mol. Biol.* **127**, 149–162 (1979).
24. Carey, F.A. & Sundberg, R.J. *Advanced organic chemistry part A: structure and mechanism* (Plenum Press, New York; 1990).
25. Ajandouz, E.H. & Marchis-Mouren, G.J. *Carbohydr. Res.* **268**, 267–277 (1995).
26. Boel, E. *et al. Biochemistry* **29**, 6244–6249 (1990).
27. Barak, D. *et al. J. Am. Chem. Soc.* **119**, 3157–3158 (1997).
28. Wind, R.D., Uitdehaag, J.C.M., Buitelaar, R.M., Dijkstra, B.W. & Dijkhuizen, L. *J. Biol. Chem.* **273**, 5771–5779 (1998).
29. Kabsch, W. *J. Appl. Crystallogr.* **21**, 916–924 (1988).
30. Otwinowski, Z. DENZO in *Data collection and Processing* (eds Sawyer, L., Isaacs, N. & Bailey, S.) 56–62 (SERC Laboratory, Daresbury, UK; 1993).
31. Jones, T.A., Zou, J.Y., Cowan, S.W. & Kjeldgaard, M. *Acta Crystallogr. A* **47**, 110–119 (1991).
32. Tronrud, D.E., Ten Eyck, L. & Matthews, B.W. *Acta Crystallogr. A* **43**, 489–501 (1987).
33. Laskowski, R.A., MacArthur, M.W., Moss, D.S. & Thornton, J.M. *J. Appl. Crystallogr.* **26**, 283–291 (1993).
34. Hooft, R.W.W., Vriend, G., Sander, C. & Abola, E.E. *Nature* **381**, 272–272 (1996).
35. Jeffrey, G.A. *Acta Crystallogr. B* **46**, 89–103 (1990).
36. Brünger, A.T. Free R value: cross-validation in crystallography. *Methods Enzymol.* **277**, 366–396.
37. Vellieux, F.M.D. & Dijkstra, B.W. *J. Appl. Crystallogr.* **30**, 396–399 (1997).
38. Read, R.J. *Acta Crystallogr. A* **42**, 140–149 (1986).
39. Kraulis, P.J. *J. Appl. Crystallogr.* **24**, 946–950 (1991).